0026-895X/08/7302-349–358$20.00
MOLECULAR PHARMACOLOGY
Copyright © 2008 The American Society for Pharmacology and Experimental Therapeutics
Mol Pharmacol 73:349–358, 2008

Vol. 73, No. 2
38877/3296798
Printed in U.S.A.

Characterization of G-Protein Coupled Receptor Kinase Interaction with the Neurokinin-1 Receptor Using Bioluminescence Resonance Energy Transfer[S]

Rasmus Jorgensen, Nicholas D. Holliday, Jakob L. Hansen, Milka Vrecl, Anders Heding, Thue W. Schwartz, and Christian E. Elling

7TM Pharma A/S, Horsholm, Denmark (R.J., A.H., T.W.S., C.E.E.); Institute of Cell Signaling, Queen's Medical Centre, Nottingham, United Kingdom (N.D.H.); Institute of Anatomy, Histology, and Embryology, Veterinary Faculty, University of Ljubljana, Slovenia (M.V); Laboratory for Molecular Pharmacology, The Panum Institute 18.6, University of Copenhagen, Copenhagen, Denmark (J.L.H., T.W.S.); and Laboratory for Molecular Cardiology, the Danish National Research Foundation Centre for Cardiac Arrhythmia, the Heart Centre, Copenhagen University Hospital, Copenhagen, Denmark (J.L.H.).

Received June 7, 2007; accepted November 6, 2007

ABSTRACT

To analyze the interaction between the neurokinin-1 (NK-1) receptor and G-protein coupled receptor kinases (GRKs), we performed bioluminescence resonance energy transfer^2 (BRET^2) measurements between the family A NK-1 receptor and GRK2 and GRK5 as well as their respective kinase-inactive mutants. We observed agonist induced interaction of both GRK5 and GRK2 with the activated NK-1 receptor. In saturation experiments, we observed GRK5 to interact with the activated receptor in a monophasic manner while GRK2 interacted in a biphasic manner with the low affinity phase corresponding to receptor affinity for GRK5. Agonist induced GRK5 interaction with the receptor was dependent on intact kinase-activity, whereas the high affinity phase of GRK2 interaction was independent of kinase activity. We were surprised to find that the BRET^2 saturation experiments indicated that before receptor activation, the full-length NK-1 receptor, but not a functional C-terminal tail-truncated receptor, is preassociated with GRK5 in a relatively low-affinity state. We demonstrate that GRK5 can compete for agonist induced GRK2 interaction with the NK-1 receptor, whereas GRK2 does not compete for receptor interaction with GRK5. We suggest that GRK5 is preassociated with the NK-1 receptor and that GRK5, rather than GRK2, is a key player in competitive regulation of GRK subtype specific interaction with the NK-1 receptor.

Seven transmembrane (7TM) G-protein-coupled receptors interact with heterotrimeric G-proteins upon activation. Receptor activation results in initiation of G-protein mediated signal transduction cascades leading to up- or down-regulation of intracellular levels of secondary messengers such as cAMP, inositol trisphosphate, or Ca^{2+}. Termination of the receptor-mediated signaling is regulated by second messenger+regulated kinases and G-protein-coupled receptor kinases (GRKs). GRK-mediated phosphorylation of the receptor promotes receptor recruitment of the intracellular scaffolding proteins βarrestins (βarrs) from the cytosol, thereby excluding the receptor from further G-protein interaction (Luttrell and Lefkowitz, 2002). In addition to uncoupling 7TM receptors from G-proteins, βarrs recruit the receptor to clathrin-coated pits (Goodman et al., 1996) and initiates signaling pathways such as mitogen-activated protein kinase cascades (Luttrell and Lefkowitz, 2002). Seven members of the mammalian GRK family have so far been described. These GRKs are classified in three subgroups based on sequence homology and function: the visual GRK1 and -7, nonvisual cytosolic GRK2 and -3, and nonvisual membrane-associated GRKs 4, 5, and 6. With GRK4 as the exception, nonvisual GRKs are rather ubiquitously expressed in mammalian tissues. Although very little is known about GRK subtype-specific phosphorylation patterns of 7TM receptors, recent publications report GRK subtype-specific initiation of cellular events (Kim et al., 2005;

J.L.H. was supported by The Danish Medical Research Council and the Danish National Research Foundation and N.D.H. was supported by the Royal Society (UK).

Article, publication date, and citation information can be found at http://molpharm.aspetjournals.org.

doi:10.1124/mol.107.038877.

[S] The online version of this article (available at http://molpharm.aspetjournals.org) contains supplemental material.

ABBREVIATIONS: 7TM, seven transmembrane; NK-1, neurokinin-1; GRK, G-protein-coupled receptor kinase; βarr, βarrestin; BRET, bioluminescence resonance energy transfer; RLuc, *Renilla reniformis* luciferase; SP, substance P; HEK, human embryonic kidney; BSA, bovine serum albumin; PBS, phosphate-buffered saline; wt, wild type.

Ren et al., 2005). At present, it is unknown how GRK subtype-specific functional effects are obtained, and details of the interaction pattern between 7TM receptors and GRK subtypes remain largely undescribed. Protein-protein interactions have been analyzed using coimmunoprecipitation techniques. For more detailed analysis, coimmunoprecipitation has several limitations, including the necessity for lysis and detergent treatment of the cells as well as low time resolution, making it difficult to detect transient interactions. For the analysis of GRK2 and GRK5 interaction with the NK-1 receptor, we used the bioluminescence resonance energy transfer (BRET) technique because it offers a relatively high-resolution method for analysis of biological interactions in living cells (Perroy et al., 2004; Galés et al., 2005, 2006). The BRET technique has previously been employed in the analysis of GRK2 but not GRK5 interaction with 7TM receptors (Hasbi et al., 2004; Jorgensen et al., 2007).

Materials and Methods

Molecular Biology. Human βarr2 N-terminally tagged with green fluorescent protein^2 (GFP^2-βarr2) and the *Renilla reniformis* luciferase (RLuc) cDNA were purchased from PerkinElmer Life and Analytical Sciences (Waltham, MA). Human GRK2 and GRK5 cDNA were cloned from a pancreatic cDNA library (Clontech, Mountain View, CA). GFP^2 or RLuc fusions were generated using standard methods. GRK2-GFP^2-Membrane was made by inserting the cDNA sequence encoding the C-terminal 17 amino acid residues from human K-ras (KDGKKKKKKSKTKCVIMS) followed by a stop codon in a 3′ position of the GRK2-GFP^2 cDNA lacking the stop codon. Mutations were made using QuikChange site-directed mutagenesis kit (Stratagene, La Jolla, CA). All cDNA clones were verified by sequencing. Substance P (SP) peptide was obtained from Bachem (Bubendorf, Switzerland).

Transfections and Tissue Culture. cDNAs were transiently expressed in HEK293 cells transfected by calcium phosphate precipitation according to methods reported previously (Elling and Schwartz, 1996). HEK293 cells were obtained from the European Collection of Animal Cell Cultures. The cells were routinely maintained and passaged as recommended by the supplier.

Inositol Phosphate Assay. Agonist induced inositol phosphate accumulation was measured as described previously (Liu et al., 2003).

BRET^2 Assays. BRET^2 measurement was done using a Mithras LB 940 plate reader (Berthold Technologies, Bad Wildbad, Germany) as described previously (Jorgensen et al., 2007). All measurements were made at room temperature. The reading time was 5 min after agonist addition for dose-response curves. For kinetic studies, variable reading times were used, and agonist was added with an injector. For BRET^2 saturation experiments, a range of transfections were made with a stable amount of NK1R-RLuc cDNA and increasing amounts of cDNA encoding the GFP^2 fused protein. Reading times were as indicated in the figures. The background signal from Rluc was determined by coexpressing the Rluc construct with empty vector, and the BRET^2 ratio generated from this transfection was subtracted from all other BRET^2 ratios. Expression levels of Rluc- and GFP^2-tagged constructs for each BRET^2 saturation experiment were monitored by luminescence and fluorescence measurements. Luminescence was measured on the Mithras LB 940 plate reader two seconds after Deep Blue C (Coelenterazine 400a; PerkinElmer Life and Analytical Sciences) addition. For fluorescence measurements, cells from the same transfections were plated in a black clear-bottom microplate (ViewPlate; PerkinElmer Life and Analytical Sciences) at a density of $\sim 5 \times 10^4$ cells per well. After 1-h incubation in darkness, the total fluorescence was measured using the NovoStar microplate reader (BMG LabTech, Offenburg, Germany), with an excitation line at 485 nm and an emission filter at 520 nm. Background values obtained with cells transfected with the relevant RLuc construct but no GFP^2 construct were subtracted, and the means of quadruplicate wells/sample were then calculated.

Confocal Fluorescence Microscopy. HEK293T cells were grown to 50% confluence on poly-L-lysine–coated, 22-mm diameter glass coverslips and transiently transfected (Lipofectamine; Invitrogen, Paisley, UK) with the FLAG-NK1 receptor and GRK5-GFP^2, GRK2-GFP^2, or GRK2-GFP^2-Membrane cDNAs (0.5 μg + 0.5 μg per well). After 24 h, the medium was exchanged for serum-free Opti-MEM (Invitrogen) including 1% bovine serum albumin (30 min, 37°C), and the cells were then incubated for 30 min at 37°C in Opti-MEM/1% bovine serum albumin including M2 anti FLAG antibody (2.5 μg/ml, 150 μl per coverslip; Sigma, Poole, UK). Vehicle (50 μl of medium) or SP (10 nM final concentration) were added for 5 min, and cells were then washed in phosphate-buffered saline (PBS), fixed in 3% paraformaldehyde in PBS (15 min, 21°C), and permeabilized with 0.075% Triton X-100 for 5 min. Bound M2 antibody was detected by goat anti-mouse IgG conjugated to Rhodamine Red X (1:1000; Invitrogen). Cells were postfixed in 3% paraformaldehyde, and coverslips were mounted in 1:1 PBS/glycerol, sealed with nail varnish. Confocal microscopy was performed on a Zeiss LSM 510M laser-scanning microscope with a Plan-Apochromat 63× 1.4 numerical aperture oil objective. Images were acquired in multitrack mode using an argon laser line at 488 nm and bandpass emission filter at 505 to 550 nm (GRK-GFP^2), and helium-neon laser with excitation at 543 nm and a long-pass filter at 560 nm (Rhodamine Red X secondary antibody). Ten to 15 representative cells were scanned for each data group, using gain and offset adjustments to obtain a full range of image intensities without saturation. Channel acquisition parameters were similar in the control and SP-treated examples given in Fig. 5.

Calcium Measurements. Calcium measurements were made using the NovoStar microplate reader (BMG LabTech, Offenburg, Germany) as described previously (Kubale et al., 2007).

Receptor Internalization. NK-1 receptor internalization was measured using the acid wash method with ^{125}I-SP tracer (GE Healthcare, Chalfont St. Giles, Buckinghamshire, UK) as described previously (Kubale et al., 2007).

Data Analysis. Nonlinear regression analysis was made using Prism (GraphPad Software, Inc., San Diego, CA). BRET50 values were determined by one-phase exponential association or two-phase exponential association using Prism.

Results

The NK-1 receptor, a prototypical family A 7TM receptor, has been demonstrated to undergo GRK2- and GRK5-mediated phosphorylation in vitro (Nishimura et al., 1998; Walker et al., 1999). However, the interaction pattern of the receptor and the GRKs in living cells has not been described. To analyze the interactions between the NK-1 receptor and GRK2 and GRK5, respectively, we employed a BRET assay in transfected HEK293 cells. The BRET assay is a proximity based assay that measures energy transfer from an Rluc-tagged protein to a GFP-tagged protein upon addition of the Rluc substrate Deep Blue C (Mercier et al., 2002; Milligan, 2004). The BRET signal is highly distance-dependent and is obtained if the Rluc energy donor and the GFP acceptor are within approximately ≤100 Å of each other. We measured BRET^2 by using the GFP^2 blue-shifted variant of GFP. We tagged the NK-1 receptor C-terminally with RLuc (NK1R-RLuc) and the GRKs C-terminally with GFP^2 (GRK2-GFP^2 and GRK5-GFP^2). Functional expression of the NK1R-RLuc construct has been demonstrated (Vrecl et al., 2004), and other reports use GRK2 and GRK5 with C-terminal tags

(Schulz et al., 2002; Li et al., 2003; Hasbi et al., 2004; Thiyagarajan et al., 2004; Jorgensen et al., 2007).

To further validate the functionality of GFP^2-tagged GRK constructs and to analyze the ability of GRKs to regulate NK-1 receptor signaling, we measured the ability of the NK-1 receptor to mediate agonist induced inositol phosphate accumulation after coexpression with either vector, GRK2, GRK2-GFP^2, GRK2(K220R), GRK2(K220R)-GFP^2, GRK5, GRK5-GFP^2, GRK5(K215R), or GRK5(K215R)-GFP^2. The GRK2(K220R) and GRK5(K215R) mutants have been demonstrated to be kinase-inactive and are in some reports described to be dominant-negative (Kong et al., 1994; Diviani et al., 1996; Pronin and Benovic, 1997; Tiruppathi et al., 2000). We observed that coexpression of the NK-1 receptor with either GRK2 construct caused a substantial attenuation of agonist-induced inositol phosphate accumulation (Fig. 1A), demonstrating that GRK2 can regulate NK-1 receptor signaling and that the GFP^2 fused GRK2 is functional. Furthermore, the ability of the kinase-inactive GRK2 mutants to attenuate NK-1 receptor-mediated signaling indicates that GRK2 can exert a phosphorylation-independent effect on receptor signaling. When measuring receptor-mediated inositol phosphate accumulation in the presence of coexpressed GRK5 constructs, we found that both GRK5 and GRK5-GFP^2 coexpression attenuated receptor signaling to a similar level, suggesting that GRK5 can regulate NK-1 receptor signaling and that GFP^2-fused GRK5 remains functional (Fig. 1B). Coexpression of the kinase-inactive GRK5(K215) mutant seemed to cause a relatively modest attenuation of NK-1 receptor-mediated inositol phosphate accumulation (Fig. 1B). However, the effect was not significant (Student's *t* test) and was not observed with GFP^2-fused GRK5(K215R) construct, suggesting that GRK5 does not exert phosphorylation-independent effects on NK-1 receptor signaling.

To further distinguish phosphorylation-dependent and -independent effects of GRK2 and GRK5 on NK-1 receptor signaling, we employed a naturally occurring splice variant of the NK-1 receptor in which all of the receptor tail C-terminal to the palmitoylated Cys is lacking (Richardson et al., 2003) The NK1R(1–324) variant (numbers referring to remaining amino acid residues) has been reported not to be phosphorylated and to have reduced ability to interact with βarrs (Oakley et al., 2001; Richardson et al., 2003). We measured the ability of the tail-truncated NK-1R(1–324) construct to mediate agonist induced inositol phosphate accumulation when coexpressed with either vector, GRK5, GRK5-GFP^2, GRK2, or GRK2-GFP^2 (Fig. 1C). Coexpression of GRK5 or GRK5-GFP^2 did not influence the signaling of the NK-1R(1–324) construct, whereas GRK2 and GRK2-GFP^2 coexpression attenuated NK-1R(1–324)–mediated inositol phosphate accumulation, although to a lesser degree than observed with the wild+type receptor [maximal signal with GRK2 coexpression relative to control was 2% and 28% for NK1R(wt) and NK1(1–324), respectively]. Thus, the data suggest that the GRK5 effect on NK-1 receptor signaling was dependent on intact GRK5 kinase activity and on the presence of the receptor C-terminal tail, whereas GRK2 seems to have both phosphorylation-dependent and -independent effects on NK-1 receptor signaling.

To ensure that the NK-1 receptor is not constitutively desensitized when coexpressed with GRK2 or GRK5, we analyzed whether the receptor could generate a calcium signal in the initial 50 s after agonist addition. As seen in Fig. 2 both wild-type NK-1 receptor and NK1R-RLuc coexpressed with either vector, GRK2, or GRK5 mediates a calcium signal immediately after agonist addition. Thus, GRK coexpression does not cause constitutive desensitization of the NK-1 receptor, although a suppression of the max signal is observed in the presence of GRK coexpression (Fig. 2). As the time-dependent decrease of the peak in agonist-induced calcium signal reflects receptor desensitization as well as postreceptor mechanisms, we normalized the signals to percentage of maximum signal for optimal comparison (Fig. 2, inset) (Kubale et al., 2007). Coexpression of GRK2 or GRK5 caused the calcium signal to decrease with faster kinetics relative to

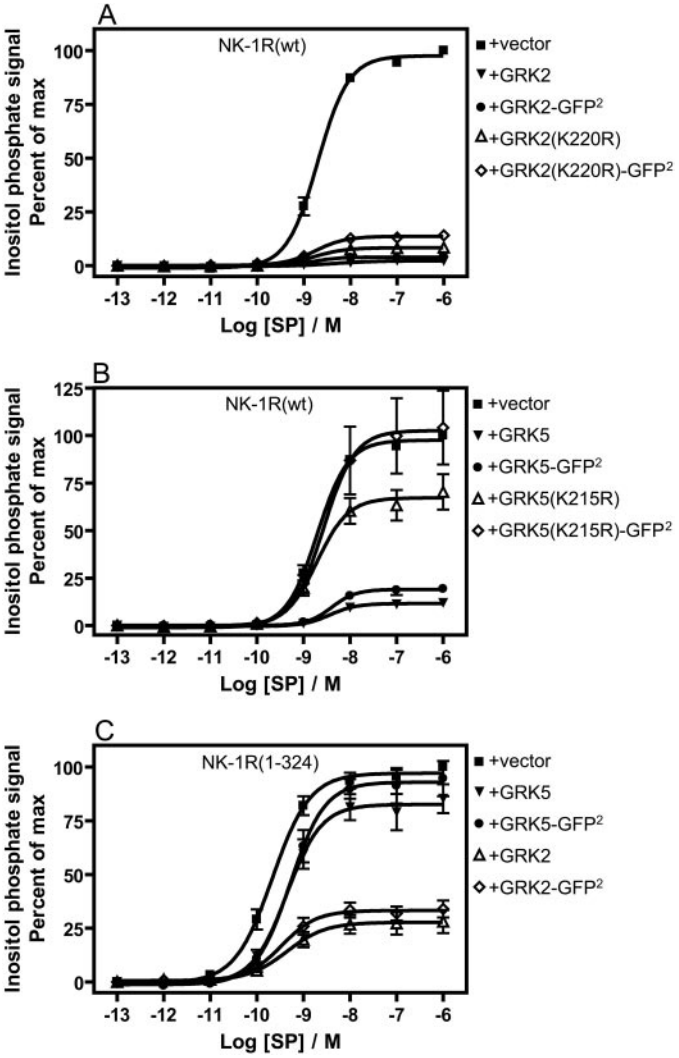

Fig. 1. Agonist-induced inositol phosphate accumulation. Dose response curves for agonist-induced inositol phosphate accumulation in HEK293 cells transiently transfected with cDNA encoding the NK-1 receptor and the indicated cDNAs. A, SP induced inositol phosphate accumulation in cells with NK-1 receptor coexpressed with either vector, GRK2, GRK2-GFP^2, GRK2(K220R), or GRK2(K220R)-GFP^2. B, SP induced inositol phosphate accumulation in cells with NK-1 receptor coexpressed with either vector, GRK5, GRK5-GFP^2, GRK5(K215R), or GRK5(K215R)-GFP^2. C, SP induced inositol phosphate accumulation in cells with tail truncated NK-1(1–324) receptor coexpressed with either vector, GRK5, GRK5-GFP^2, GRK2, or GRK2-GFP^2. The response is expressed as percent of the maximal response for the receptor cotransfected with empty vector. The curve for NK-1R+vector in A and B is identical. Results are the means ± S.E.M. of duplicate determinations in three independent experiments.

coexpression with vector, indicating that the receptor desensitizes faster when GRKs are coexpressed (Fig. 2, inset). Furthermore, the data suggest that the NK1R-RLuc fusion is comparable with NK-1R(wt) in the ability to generate an agonist-induced calcium signal (Fig. 2).

We next assessed the interaction between NK1R-RLuc and GRK5-GFP^2 in transfected HEK293 cells by analyzing the BRET^2 signal at progressive time points after addition of 10 nM SP—an agonist concentration that we found to have full efficacy in inducing recruitment of βarr2 to the NK-1 receptor (Supplementary Fig. 1). When measuring BRET^2 between NK1R-RLuc and GRK5-GFP^2, we observed a relatively high basal signal that increased to reach a transient peak at ~20 s after agonist addition and returned to basal after ~1 min (Fig. 3A). To analyze the interaction between the NK-1 receptor and GRK5 in more detail, we performed BRET^2 saturation experiments. In these experiments, the amount of the GFP^2-fused protein is gradually increased relative to a steady amount of the RLuc-fused protein (Mercier et al., 2002; Galés et al., 2006). In case of a specific interaction between the tagged proteins, the BRET^2 signal should display a hyperbolic curve as a function of the GFP^2/RLuc expression ratio (Mercier et al., 2002; Galés et al., 2006). In contrast, nonspecific background arising from random collisions of the tagged proteins ("bystander BRET") should result in a BRET^2 signal that depends linearly on the GFP^2/RLuc expression ratio (Mercier et al., 2002; Galés et al., 2006). We observed a hyperbolic curve between GRK5-GFP^2 and the NK1R-RLuc, indicating that there is a basal association of GRK5 with the resting (i.e., receptor before agonist exposure) NK-1 receptor (Fig. 3B). The GFP/RLuc ratio resulting in half-maximal saturation is referred to as the BRET50 value and is a measure of the affinity in arbitrary units (Mercier et al., 2002; Galés et al., 2006). Hence, BRET^2 saturation experiments are suitable for comparing affinities on a relative scale. Twenty seconds of receptor stimulation with 10 nM SP (corresponding to the time point of the peak in the BRET^2 signal between GRK5-GFP^2 and NK1R-RLuc) caused the curve to saturate with a lower BRET50 value, reflecting increased affinity of GRK5 for the receptor (BRET50 values of 0.19 and 0.48 with and without agonist addition, respectively). Thus, the BRET^2 saturation data are consistent with the time course experiments and demonstrate that GRK5 is recruited during receptor activation to form a closer complex with the NK-1 receptor ~20 s after receptor activation. Because some random interaction will occur between any proteins it was important to control that the apparent specific interaction between GRK5 and the resting receptor did not simply arise from bystander BRET^2 between two membrane-localized proteins. The tail-truncated NK-1(1–324), which, in the inositol phosphate signaling assay, was observed to be signaling competent but not regulated by GRK5, was C-terminally RLuc tagged for the experiments (NK1R(1–324)-RLuc). The NK1R(1–324)-RLuc construct mediated agonist induced inositol phosphate accumulation virtually similar to the full-length NK1R-RLuc, demonstrating also that the RLuc-fused tail-truncated receptor construct was expressed and signaling competent (Supplementary Fig. 2). When performing BRET^2 saturation experiments with the truncated NK1R(1–324)-RLuc construct and GRK5-GFP^2, we observed a linear curve as a function of the GFP^2/RLuc ratio both before and after agonist addition, suggesting that the NK1R(1–324)-RLuc construct did not interact with GRK5 (Fig. 3B). Furthermore, this suggested that the BRET^2 signal between NK1R-RLuc and GRK5-GFP^2 was not simply caused by both proteins being localized to the membrane. We further proceeded to characterize the interaction pattern of the kinase inactive GRK5(K215R) mutant with the NK-1 receptor. We were surprised to find that when performing time-course experiments with NK1R-RLuc and GRK5(K215R)-GFP^2, we observed no agonist-induced increase in the BRET^2 signal but rather a time-dependent decrease in the signal, reaching a plateau ~1 min after agonist addition (Fig. 3C). Furthermore, the basal BRET^2 signal was higher than observed with the NK1R-RLuc/GRK5-GFP^2 combination (Fig. 3). When performing BRET^2 saturation experiments with the NK1R-RLuc and GRK5(K215R)-GFP^2, we observed the BRET^2 signal, without agonist addition, to describe a slightly hyperbolic curve as a function of the GRK5(K215R)-GFP^2/NK1R-RLuc ratio (Fig. 3D). Compared with GRK5-GFP^2 interaction with NK1R-RLuc, the basal BRET^2 signal for GRK5(K215R)-GFP^2 was higher over a range of expression ratios, but it did not reflect a higher affinity phenotype (Fig. 3, B and D). Twenty seconds after addition of the agonist SP, the maximum BRET^2 signal decreased without concomitant changes in the shape of the curve (Fig. 3D). Thus, the BRET^2 data suggest that the GRK5(K215R) mutant is organized in a low affinity association with the resting NK-1 receptor and that the mutant is not further recruited to the receptor after receptor activation.

We proceeded by characterizing the interaction between

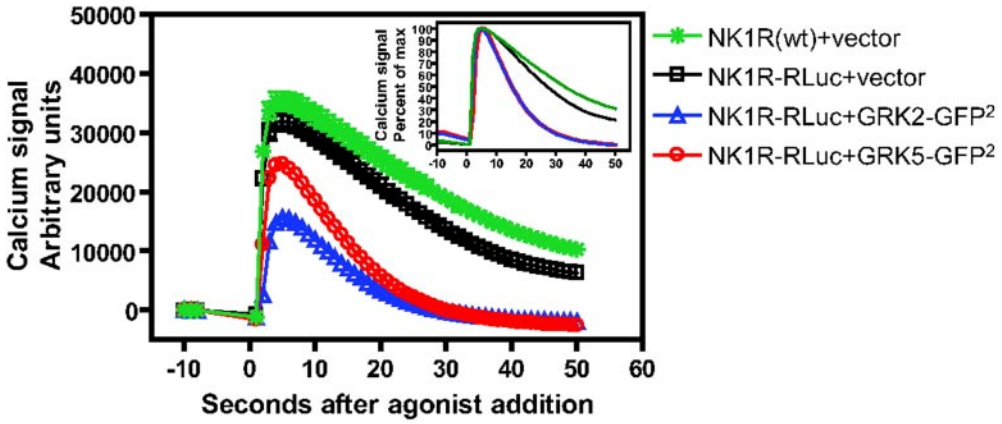

Fig. 2. Agonist-induced calcium signal. Kinetics of agonist (10 nM SP)-induced calcium signal in transiently transfected HEK293 cells. The cells were either transfected with cDNAs encoding NK1R(wt)+ vector or NK1R-RLuc cotransfected with vector, GRK2-GFP^2, or GRK5-GFP^2 as indicated (cDNA ratio of 1:2). The inserted figure shows the signals normalized to percent of maximal generated calcium signal for each transfection condition. Data represents the mean ± S.E.M. for a single experiment carried out in sextuplicate determinations and are representative of a total of three independent experiments.

the NK-1 receptor and GRK2. When performing BRET^2 time course experiments with NK1R-RLuc and GRK2-GFP^2 we observed a rapid recruitment of GRK2-GFP^2 to the NK1R-RLuc (Fig. 4A). The signal peaked transiently at 10 to 20 s after agonist addition and then stabilized at a lower level (Fig. 4A). When performing BRET^2 saturation experiments, the BRET^2 signal after agonist addition described a hyperbolic curve as a function of GRK2-GFP^2/NK1R-RLuc that was best fit with a two-phase exponential association model (BRET50 values of 0.015 and 0.17 for the high- and low-affinity phases, respectively, measured 5 min after agonist addition) (Fig. 4B). It is noteworthy that the curve after 20 s of agonist addition (corresponding to the peak in the BRET^2 signal in the time course measurements) was similar to the curve after 5 min of agonist addition, suggesting that the transient peak does not describe a higher affinity phenotype of the GRK2/NK-1 receptor complex relative to the signal plateau (Fig. 4B). As a control, we performed BRET^2 saturation experiments with GRK2-GFP^2 and the receptor tail truncated NK1R(1–324)-RLuc. Without agonist addition, the BRET^2 signal displayed a linear curve as a function of the GRK2-GFP^2/NK1R(1–324)-RLuc (Fig. 4B). Twenty seconds of agonist addition caused a slight increase in BRET^2 signal, which may suggest that there is a low level of agonist-dependent GRK2 recruitment to the NK1R(1–324) (Fig. 4B). To analyze the dependence of GRK2 kinase activity for the observed interaction with the NK-1 receptor, we performed BRET^2 time-course experiments of NK1R-RLuc interaction with the kinase inactive GRK2 mutant GRK2(K220R)-GFP^2 after addition of 10 nM SP. In contrast to the results obtained with GRK5, the kinase inactive GRK2(K220R) mutant was recruited to the activated NK-1 receptor in a pattern similar to the wild-type GRK2 (Fig. 4C). We proceeded by performing BRET^2 saturation experiments with GRK2(K220R)-GFP^2 and NK1R-RLuc. We observed GRK2(K220R) interaction with the NK-1 receptor to saturate in a monophasic manner with a BRET50 value of 0.019 corresponding to the high-affinity phase of GRK2 interaction with the NK-1 receptor (Fig. 4D). Thus, the biphasic nature of the BRET^2 saturation curve for GRK2 interaction with the NK-1 receptor seemed to consist of kinase-independent and -dependent phases.

To analyze whether the difference in phenotype of GRK2 and GRK5 interaction with the NK-1 receptor depends on the difference in cellular localization of the two GRKs, we made a membrane localized GRK2-GFP^2 (GRK2-GFP^2-Membrane) by fusing the C-terminal 17 amino acid residues from human K-ras to the C terminus of GRK2-GFP^2. This sequence contains a polybasic signal and a prenylation sequence that in combination ensure localization to the plasma membrane (Hancock et al., 1991). We observed coexpression with GRK2-GFP^2-Membrane to suppress NK-1 receptor-mediated inositol phosphate accumulation to less than 1% of control, demonstrating that the construct was functional (data not shown). The BRET^2 signal was observed to saturate in a monophasic manner as a function of GRK2-GFP^2-Membrane/NK1R-RLuc (Fig. 4E). After agonist addition, the saturation

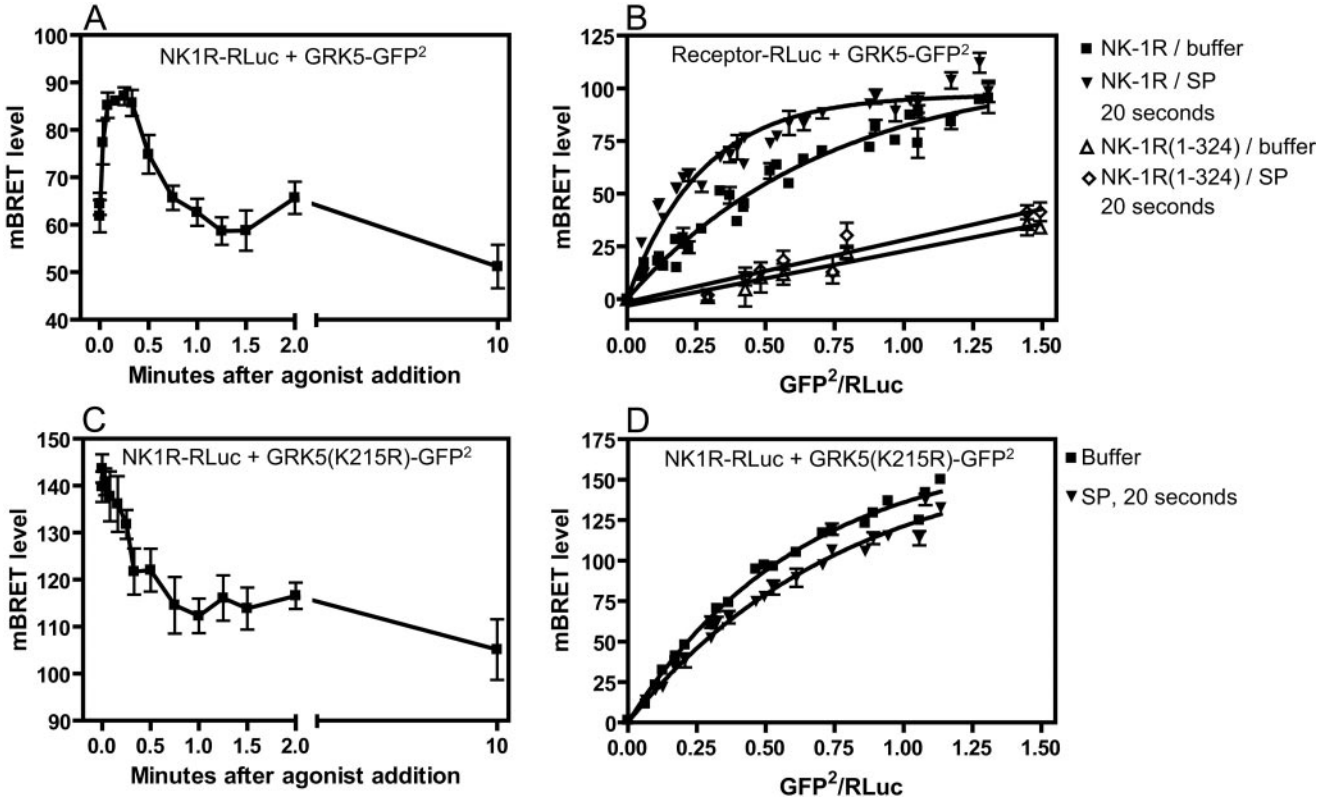

Fig. 3. BRET^2 measurements with the NK-1 receptor and GRK5 constructs. A, time course of GRK5-GFP^2 interaction with NK1R-RLuc after the addition of 10 nM SP. B, BRET^2 saturation experiments with increasing amounts of GRK5-GFP^2 relative to either NK1R-RLuc or NK1R(1–324)-RLuc. Measurements were made without receptor stimulation (buffer) or stimulation with 10 nM SP for 20 s. C, time course of GRK5(K215R)-GFP^2 interaction with NK1R-RLuc after the addition of 10 nM SP. D, BRET^2 saturation experiments with increasing amounts of GRK5(K215R)-GFP^2 relative to NK1R-RLuc. Measurements were made without receptor stimulation (buffer) or stimulation with 10 nM SP for 20 s. A and C, results are the means ± S.E.M. of duplicate determinations in at least four independent experiments. B and D, data are pooled from at least three independent experiments.

curve was best fit with a two-phase exponential association model ($p = 0.0005$) with the additional high-affinity phase as the minor phase (Fig. 4E, inset). Thus, when GRK2 is artificially membrane-localized, it displays basal interaction with the NK-1 receptor, but some agonist-induced recruitment can still be observed.

Because the BRET^2 data did not reveal where in the cell an interaction occured, we performed confocal microcopy with a FLAG-tagged NK-1 receptor and either GRK5-GFP^2 or GRK2-GFP^2 to see whether the proteins dissociate after receptor internalization. We observed the unstimulated NK-1 receptor to be localized to the plasma membrane in a clustered pattern (Fig. 5, B and C). As expected, GRK5-GFP^2 was also membrane-localized, and some clustering was observed in a pattern overlapping NK-1 receptor localization (Fig. 5, A and C). After 5 min of stimulation with 10 nM SP, extensive NK-1 receptor internalization was observed without concomitant internalization of GRK5 (Fig. 5, D–F). Thus, GRK5

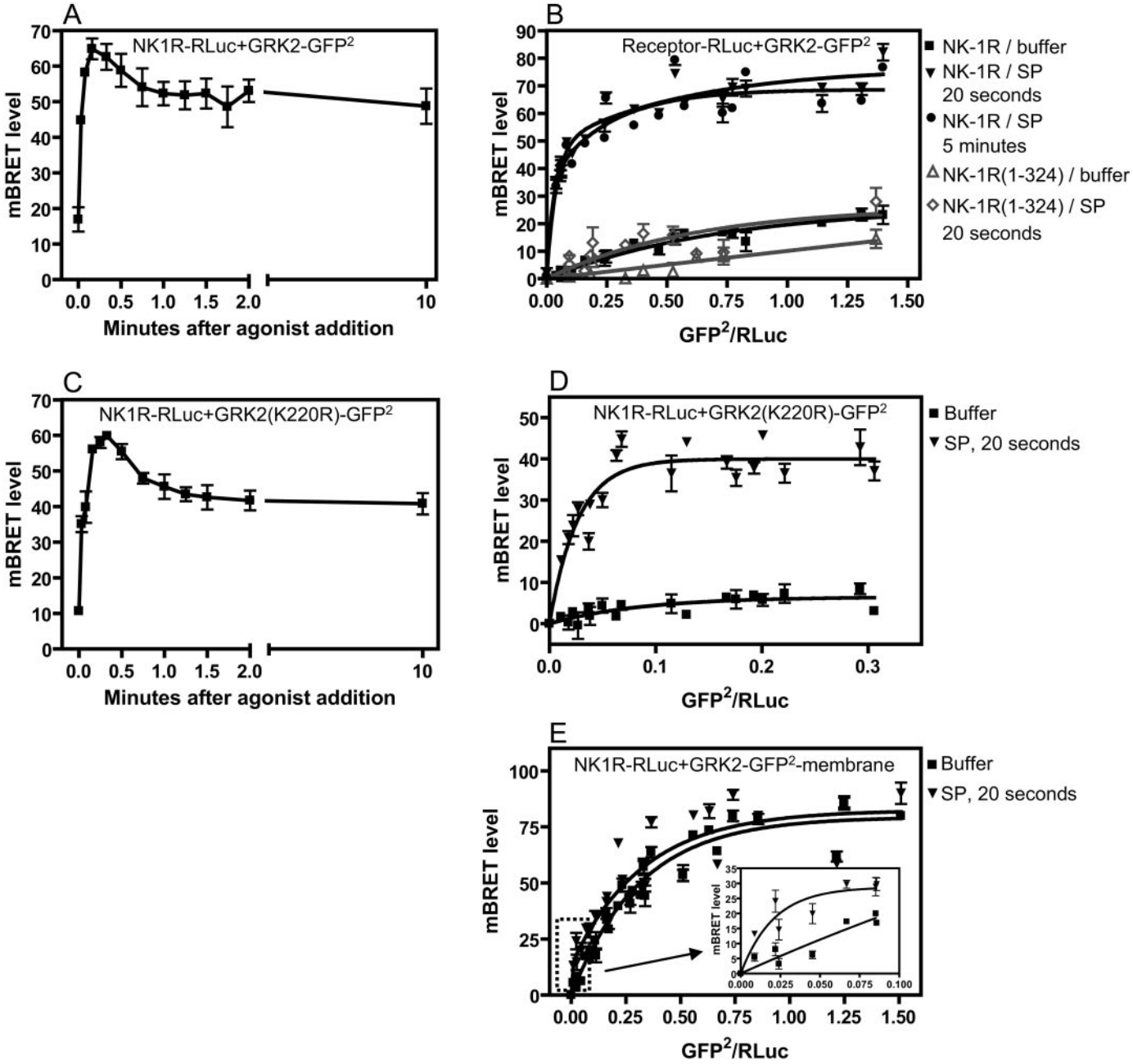

Fig. 4. BRET^2 measurements with the NK-1 receptor and GRK2 constructs. A, time course of GRK2-GFP^2 interaction with NK1R-RLuc after the addition of 10 nM SP. B, BRET^2 saturation experiments with increasing amounts of GRK2-GFP^2 relative to either NK1R-RLuc or NK1R(1–324)-RLuc. Measurements were made without receptor stimulation (buffer) or stimulation with 10 nM SP for 20 s or 5 min. C, time course of GRK2(K220R)-GFP^2 interaction with NK1R-RLuc after the addition of 10 nM SP. D, BRET^2 saturation experiments with increasing amounts of GRK2(K220R)-GFP^2 relative to NK1R-RLuc. Measurements were made without receptor stimulation (buffer) or stimulation with 10 nM SP for 20 s. E, BRET^2 saturation experiments with increasing amounts of GRK2-GFP^2-Membrane relative to NK1R-RLuc. Measurements were made without receptor stimulation (buffer) or stimulation with 10 nM SP for 20 s. Inset in E shows amplification of the areas of the curve marked with a dotted box. A and C, results are the means ± S.E.M. of duplicate determinations in at least three independent experiments. B, D, and E, data are pooled from at least three independent experiments.

colocalizes with the NK-1 receptor in membrane clusters, but it does not cointernalize with the receptor. When FLAG-NK1R was coexpressed with GRK2-GFP^2, we again observed extensive receptor internalization (Supplementary Fig. 3). Although GRK2-GFP^2 did not seem to cointernalize with the receptor, the cytoplasmic localization of GRK2-GFP^2 made it difficult to conclude on this issue (Supplementary Fig. 3). Therefore, we took advantage of the membrane localization of the GRK2-GFP^2-Membrane construct to analyze the internalization pattern. We observed GRK2-GFP^2-Membrane to be localized to the plasma membrane as expected (Fig. 5G). Although surface localization of FLAG-NK1R before agonist addition was still observed when coexpressed with GRK2-GFP^2-Membrane, there was relatively more constitutively internalized receptor compared with coexpression with GRK5-GFP^2 or GRK2-GFP^2 (compare Fig. 5, B and H, and supplementary Fig. 3B). After 5 min of agonist exposure, the receptor internalized without any apparent concomitant internalization of GRK2-GFP^2-Membrane (Fig. 5, J–L). Hence, GRK2-GFP^2-Membrane seems to increase constitutive internalization of the NK-1 but does not cointernalize with the receptor.

To analyze the influence of receptor internalization on the observed pattern of GRK2 and GRK5 interaction with the NK-1 receptor, we performed BRET^2 time course experiments in the presence 450 mM sucrose to inhibit receptor internalization (Heuser and Anderson, 1989). The BRET^2 assay was not affected by addition of sucrose to the assay buffer (data not shown). In a control experiment, we found 450 mM sucrose to significantly inhibit the kinetics of agonist-induced NK-1 receptor internalization and to inhibit the maximal internalization (Supplementary Fig. 4). Five minutes after agonist addition, hypertonic sucrose caused ~65% inhibition of receptor internalization relative to control (Supplementary Fig. 4). Both when measuring GRK5-GFP^2 and GRK2-GFP^2 recruitment to NK1R-RLuc (Fig. 6, A and B, respectively), we found the addition of sucrose in the buffer to cause a considerable increase in the basal BRET^2 signal. However, the pattern of the agonist-induced BRET^2 signal as a function of time did not differ between the experiments with or without addition of sucrose to the buffer. Thus, the observed decrease of the peak BRET^2 signal between the NK-1 receptor and GRK5 or GRK2 in time-course experiments seems to be independent of receptor internalization.

Because it is unknown whether GRK subtypes compete directly for the receptor substrate, we performed BRET^2 competition experiments. In these experiments, an untagged protein is coexpressed with the pair of tagged proteins to analyze for competition (Marullo and Bouvier, 2007). To analyze for competition of GRK5 recruitment to the NK-1 receptor, we coex-

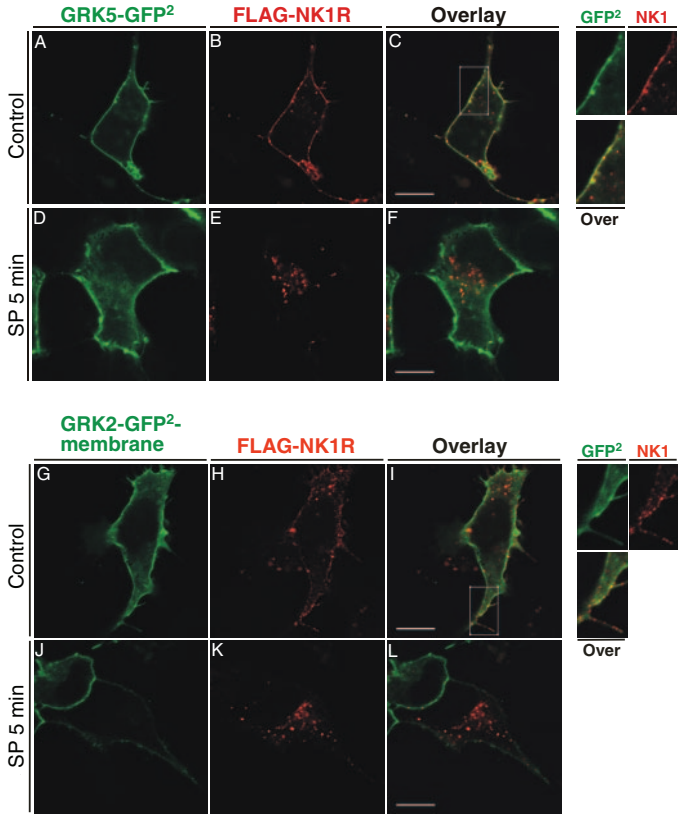

Fig. 5. Confocal microscopy in HEK293 cells coexpressing FLAG-NK-1 receptor and either GRK5-GFP^2 (A–F) or GRK2-GFP^2-Membrane (G–L). Visualization of GRK5-GFP^2 (A and D) or FLAG-NK-1 receptor (B and E) in coexpressing cells that have been stimulated with either vehicle (A–C) or 10 nM SP (D–F) for 5 min at 37°C. C and F are overlays of A plus B and D plus E, respectively. Visualization of GRK2-GFP^2-Membrane (G and J) or FLAG-NK-1 receptor (H and K) in coexpressing cells that have been stimulated with either vehicle (G–I) or 10 nM SP (J–L) for 5 min at 37°C. I and L are overlays of G plus H and J plus K, respectively. Panels to the right of C and I represent amplifications of the areas marked with a white box in the respective panels. White bars correspond to a 10-μm scale.

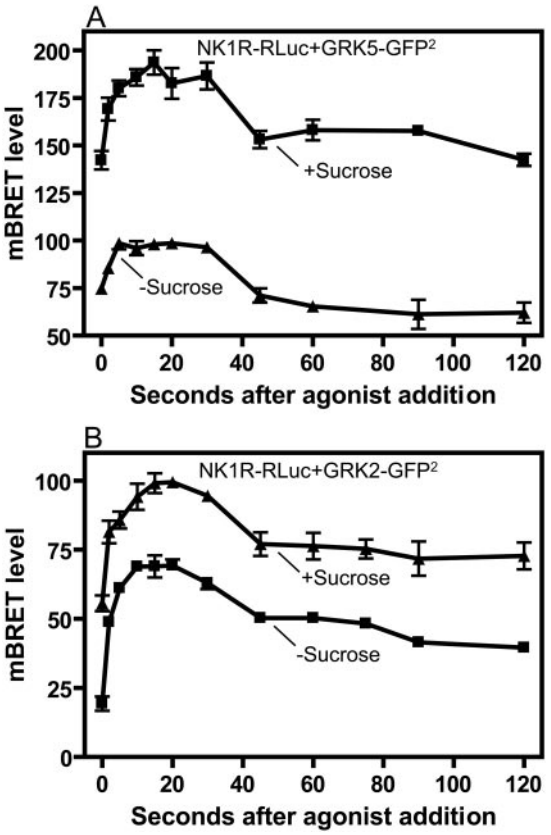

Fig. 6. Effect on BRET^2 signals of inhibition of receptor internalization by hypertonic sucrose. A, time course of GRK5-GFP^2 interaction with NK1R-RLuc after the addition of 10 nM SP with or without addition of 450 mM sucrose to the assay buffer as indicated. B, time course of GRK2-GFP^2 interaction with NK1R-RLuc after the addition of 10 nM SP with or without addition of 450 mM sucrose to the assay buffer as indicated. Results are the means ± S.E.M. of duplicate determinations in three independent experiments.

pressed NK1R-RLuc with GRK5-GFP^2 and either vector, GRK2(wt), GRK2(K220R), GRK5(wt), or GRK5(K215R) (Fig. 7A). It is noteworthy that only GRK5(wt) competed for agonist-induced GRK5-GFP^2 interaction with NK1R-RLuc (Fig. 7A). The ratio of GFP^2/RLuc did not significantly differ between the transfection conditions and was within the saturated range (range of GFP^2/RLuc was 0.61–0.86) (Supplementary Fig. 5A). When analyzing the ability of untagged proteins to compete for agonist-induced recruitment of GRK2-GFP^2 to NK1R-RLuc, we found both GRK2(wt), GRK2(K220R), GRK5(wt), and GRK5(K215R) to compete (Fig. 7B). Compared with GRK2(wt), GRK2(K220R), and GRK5(wt), untagged GRK5(K215R) was far less efficacious in the ability to compete for agonist-induced recruitment of GRK2-GFP^2 to NK1R-RLuc, and the competition only reached significance at time points 20 and 45 s after agonist addition (Fig. 7B). The range of GFP^2/RLuc was 0.83–1.39 (plus vector = 1.1) and thus within the saturated area (Supplementary Fig. 5B).

Discussion

We here characterize the interaction pattern of GRK2 and GRK5 with the NK-1 receptor. Although the role of GRKs in phosphorylating activated 7TM receptors, thereby promoting binding of βarrs, is well established (Luttrell and Lefkowitz, 2002; Pao and Benovic, 2002), details of the interaction pattern of GRK subtypes with a 7TM receptor have never been compared.

In the analysis of GRK effect on NK-1 receptor inositol phosphate signaling, we observed both GRK2 and GRK5 to attenuate NK-1 receptor signaling. It is noteworthy that GRK2 seemed to have a kinase-independent effect on NK-1 receptor signaling. In contrast, the observed effect of GRK5 on NK-1 receptor signaling seemed to be kinase-dependent. A kinase-independent effect of GRK2 is not unprecedented in that GRK2 and GRK3, in several instances, have been reported to exert phosphorylation-independent roles in 7TM receptor desensitization (Pao and Benovic, 2002). GRK2 and -3 (but not GRK5) can bind G-protein G$\alpha_{q/11}$ and G$\beta\gamma$ subunits, and the phosphorylation-independent effect on receptor desensitization is thought to originate from sequestering of these G-protein subunits and stimulation of G-protein GTPase activity (Pitcher et al., 1992; Kunapuli and Benovic, 1993; Carman et al., 1999b; Pao and Benovic, 2002). In fact, GRK2 and -3 are reported to depend on interaction with liberated G$\beta\gamma$ subunits for recruitment to activated 7TM receptors (Pitcher et al., 1992). In a BRET^2 assay, we observed limited agonist-induced interaction between a tail truncated NK-1R(1–324) construct and GRK2, which indicates that the effect of GRK2 on G-protein signaling of this receptor construct is not based on receptor interaction per se. This is consistent with the paradigm that kinase-independent effects of GRK2 are mediated by interaction with G-protein subunits rather than direct modulation of the receptor. Furthermore, the results suggest that the NK-1 receptor C-terminal tail is necessary for quantitative GRK2 interaction.

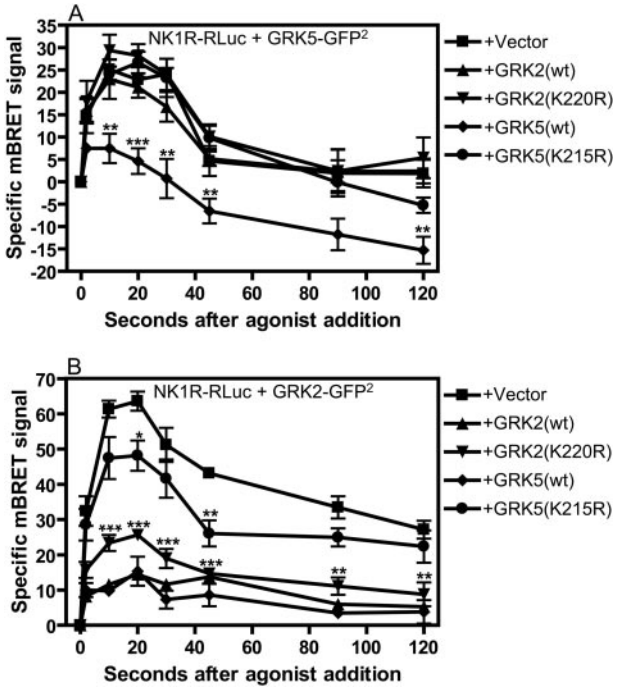

Fig. 7. BRET^2 competition experiments. Time course of GRK5-GFP^2 (A) or GRK2-GFP^2 (B) interaction with NK1R-RLuc after the addition of 10 nM SP. The cells were cotransfected with the indicated cDNAs to analyze for the ability to compete with the GFP^2-fused GRKs for NK1R-Luc interaction. Results are the means ± S.E.M. of duplicate determinations in five (A) or four (B) independent experiments. *, $p < 0.05$; **, $p < 0.01$; ***, $p < 0.001$ versus values for cotransfection with vector (unpaired Student's t test).

When analyzing GRK interaction with the NK-1 receptor, we observed several interesting differences in the GRK subtype-specific interaction patterns. Agonist-induced interaction of GRK5 with the NK-1 receptor was kinase-dependent and saturated in a monophasic manner, whereas GRK2 saturated in a biphasic manner, with the high-affinity phase being independent of kinase activity. It is possible that the high-affinity phase of GRK2 interaction with the activated NK-1 receptor represents initial GRK2 recruitment, whereas the lower affinity phase represents a conformational change promoted by phosphorylation. It is interesting to note that the monophasic interaction of GRK5 with the activated receptor seems to correspond to the kinase-dependent phase of GRK2 interaction with the receptor (BRET50 values of 0.19 and 0.17, respectively). Thus, our data suggest a difference in recruitment modes for GRK2 and GRK5 to the activated NK-1 receptor.

BRET^2 saturation experiments showed the basal BRET^2 signal for NK-1 receptor interaction to be higher, at the same expression ratios, for GRK5(K215R) compared with GRK5. Because inhibition of receptor internalization with hypertonic sucrose was observed to increase the basal BRET^2 signal, it is possible that GRK5(wt), but not GRK5(K215R), promotes constitutive phosphorylation with subsequent receptor internalization for a subpopulation of receptors, thereby decreasing the basal GRK5/NK-1 receptor BRET^2 signal. The high basal BRET^2 signal declined after receptor activation, indicating that GRK5(K215R), like GRK5(wt), is localized near the resting receptor and that dissociation/removal occurs after activation. The lack of agonist-induced receptor recruitment of GRK5(K215R) was surprising and clearly distinguishes it from the kinase-inactive GRK2-(K220R) mutant. However, in saturation experiments, GRK5 lacks the high-affinity phase of receptor interaction that is seen for GRK2 and retained in GRK2(K220R).

Our BRET^2 saturation data indicate that GRK5 is preassociated with the resting NK-1 receptor and that receptor

activation causes recruitment of GRK5 to a higher affinity complex with the receptor. The results do not allow us to distinguish between true translocation of GRK5 to the activated receptor from a nearby position (in, for example, a microdomain structure) and activation-dependent reorganization of a pre-existing GRK5/NK-1R complex. However, the BRET^2 sensitive range of ~100 Å corresponds to the diameter of only two to three 7TM receptors in the membrane plane, suggesting relatively close proximity (Palczewski et al., 2000). The notion that GRK5 may associate with resting 7TM receptors is further supported by reports that describe that overexpression of GRK5 but not GRK2 can increase basal receptor phosphorylation (Premont et al., 1994; Diviani et al., 1996; Shetzline et al., 1998, 2002). In addition, GRK5 sedimentation experiments with phospholipids versus rhodopsin-containing membranes have indicated that GRK5 can bind directly to receptors in the membrane (Pronin and Benovic, 1997). When analyzing the interaction between the NK-1 receptor and a membrane-localized GRK2 construct, we also observed an agonist-independent monophasic hyperbolic saturation curve, suggesting basal interaction. This indicates that the ability to preassociate with the NK-1 receptor depends on subcellular localization rather than properties inherent to specific GRK subtypes. However, several differences in the phenotype of GRK5 and membrane-attached GRK2 was observed. After receptor activation, the interaction of the NK-1 receptor with GRK2-GFP^2-Membrane was best fitted with a two-phase association model that corresponds to the phenotype of GRK2. Furthermore, coexpression of the NK-1 receptor and GRK2-GFP^2-Membrane was observed in confocal microscopy experiments to cause an increase in constitutive receptor internalization that was not as apparent with GRK2-GFP^2 or GRK5-GFP^2 coexpression, indicating that GRK2-GFP^2-Membrane have constitutive effects on the NK-1 receptor.

When performing confocal microscopy, we observed colocalization of GRK5 and the resting NK-1 receptor to the plasma membrane (including some clusters), and GRK5 did not cointernalize with the NK-1 receptor, thereby demonstrating that the proteins dissociate before or during receptor internalization. Likewise, we observed no cointernalization of GRK2 (or membrane-associated GRK2) and the NK-1 receptor, suggesting that the plateau in BRET^2 signal, observed in time-course experiments for GRK2 interaction with the NK-1 receptor, reflects a steady-state rather than quantitative cointernalization. After receptor internalization into cytoplasmic vesicles, increased random interaction with the cytosolic GRK2 may occur that would cause the background BRET^2 signal to increase. Inhibition of receptor internalization with hypertonic sucrose did not prevent or delay the time-dependent decrease in BRET^2 signals for agonist-dependent receptor interaction with either GRK2 or GRK5, suggesting that dissociation of GRK/NK-1R complexes occurs before receptor internalization.

BRET^2 competition experiments suggested that GRK5 can compete for agonist-induced GRK2 recruitment to the NK-1 receptor, whereas GRK2 does not compete for GRK5 recruitment to the activated receptor. This demonstrates that GRK subtypes do compete for the receptor substrate and suggests that the competition is orchestrated by more than simply relative amounts of GRK subtypes or relative affinities for the activated receptor. Indeed, the competition data would support a hypothesis that GRK5 preassociation with the NK-1 receptor, causing a local high concentration of GRK5, gives an advantage of proximity that outweighs the higher affinity of GRK2 for the activated receptor. The competition between GRK subtypes could be both steric and functional. Steric competition between large proteins that interact with the same domain of the receptor would be expected, and GRK5-mediated receptor phosphorylation and subsequent uncoupling would prevent further GRK2 recruitment because GRK2 depends on G-protein activation for translocation (Pitcher et al., 1992).

The untagged GRK2(K220R) mutant was observed to compete for GRK2-GFP^2 recruitment to the NK-1 receptor, thereby further supporting reports that the GRK2(K220R) mutant is dominant-negative (Kong et al., 1994; Diviani et al., 1996). However, as untagged GRK5(K215R), did not compete for GRK5-GFP^2 recruitment to the activated NK-1 receptor, our results do not support the use of the GRK5-(K215R) mutant as a dominant-negative tool. It remains possible that GRK5(K215) has a competitive effect on basal GRK5 preassociation with the resting receptor that we do not see in our assay. Because the GRK constructs may have an effect on constitutive receptor internalization that the basal BRET^2 signal seems to be highly sensitive to, we cannot determine whether effects of overexpressed untagged GRKs on the basal BRET^2 signal reflects competition or changes in the ratio of surface receptor/total receptor.

Our data suggest that GRK5 rather than GRK2 is a key player in the regulation of GRK subtype-specific interaction with the NK-1 receptor. Because the ability of GRK5 to regulate GRK2 interaction with the receptor seems to be largely dependent on kinase activity, one could speculate that inhibition of GRK5 kinase activity would not only prevent GRK5-mediated receptor phosphorylation but, furthermore, would allow GRK2-mediated phosphorylation. In this context, it is interesting to note that GRK5 kinase activity can be inhibited by calcium/calmodulin and structural proteins such as actin, α-actinin, and caveolin (Pronin et al., 1997; Freeman et al., 1998; Carman et al., 1999a; Freeman et al., 2000).

In conclusion, we demonstrate differences in affinity, kinase dependence, and level of basal interaction for GRK2 and GRK5 interaction with the NK-1 receptor. We suggest that, rather than relative amounts of GRK subtypes, GRK5 preassociation with the receptor is involved in the orchestration of subtype-specific GRK regulation of receptor signaling. It will be interesting to see future research delineate in more detail how the complex interaction pattern between receptors and GRKs, as well as other accessory proteins, is biologically regulated and how this contributes to the regulation of receptor signaling.

Acknowledgments

We thank Susanne Hummelgaard, Kate Hansen, Helle Zancho Andresen, and Helle Iversen for excellent technical assistance.

References

Carman CV, Lisanti MP, and Benovic JL (1999a) Regulation of G protein-coupled receptor kinases by caveolin. *J Biol Chem* **274:**8858–8864.

Carman CV, Parent JL, Day PW, Pronin AN, Sternweis PM, Wedegaertner PB, Gilman AG, Benovic JL, and Kozasa T (1999b) Selective regulation of $G\alpha_{q/11}$ by an RGS domain in the G protein-coupled receptor kinase, GRK2. *J Biol Chem* **274:** 34483–34492.

Diviani D, Lattion AL, Larbi N, Kunapuli P, Pronin A, Benovic JL, and Cotecchia S

(1996) Effect of different G protein-coupled receptor kinases on phosphorylation and desensitization of the α_{1b}-adrenergic receptor. *J Biol Chem* **271:**5049–5058.
Elling CE and Schwartz TW (1996) Connectivity and orientation of the seven helical bundle in the tachykinin NK-1 receptor probed by zinc site engineering. *EMBO J* **15:**6213–6219.
Freeman JL, De La Cruz EM, Pollard TD, Lefkowitz RJ, and Pitcher JA (1998) Regulation of G protein-coupled receptor kinase 5 (GRK5) by actin. *J Biol Chem* **273:**20653–20657.
Freeman JL, Pitcher JA, Li X, Bennett V, and Lefkowitz RJ (2000) Alpha-actinin is a potent regulator of G protein-coupled receptor kinase activity and substrate specificity in vitro. *FEBS Lett* **473:**280–284.
Galés C, Rebois RV, Hogue M, Trieu P, Breit A, Hebert TE, and Bouvier M (2005) Real-time monitoring of receptor and G-protein interactions in living cells. *Nat Methods* **2:**177–184.
Galés C, Van Durm JJ, Schaak S, Pontier S, Percherancier Y, Audet M, Paris H, and Bouvier M (2006) Probing the activation-promoted structural rearrangements in preassembled receptor-G protein complexes. *Nat Struct Mol Biol* **13:**778–786.
Goodman OB Jr, Krupnick JG, Santini F, Gurevich VV, Penn RB, Gagnon AW, Keen JH, and Benovic JL (1996) Beta-arrestin acts as a clathrin adaptor in endocytosis of the beta2-adrenergic receptor. *Nature* **383:**447–450.
Hancock JF, Cadwallader K, Paterson H, and Marshall CJ (1991) A CAAX or a CAAL motif and a second signal are sufficient for plasma membrane targeting of Ras proteins. *EMBO J* **10:**4033–4039.
Hasbi A, Devost D, Laporte SA, and Zingg HH (2004) Real-time detection of interactions between the human oxytocin receptor and G protein-coupled receptor kinase-2. *Mol Endocrinol* **18:**1277–1286.
Heuser JE and Anderson RG (1989) Hypertonic media inhibit receptor-mediated endocytosis by blocking clathrin-coated pit formation. *J Cell Biol* **108:**389–400.
Jorgensen R, Kubale V, Vrecl M, Schwartz TW, and Elling CE (2007) Oxyntomodulin differentially affects glucagon-like peptide-1 receptor β-arrestin recruitment and signaling through $G\alpha_s$. *J Pharmacol Exp Ther* **322:**148–154.
Kim J, Ahn S, Ren XR, Whalen EJ, Reiter E, Wei H, and Lefkowitz RJ (2005) Functional antagonism of different G protein-coupled receptor kinases for beta-arrestin-mediated angiotensin II receptor signaling. *Proc Natl Acad Sci U S A* **102:**1442–1447.
Kong G, Penn R, and Benovic JL (1994) A β-adrenergic receptor kinase dominant negative mutant attenuates desensitization of the β_2-adrenergic receptor. *J Biol Chem* **269:**13084–13087.
Kubale V, Abramovic Z, Pogacnik A, Heding A, Sentjurc M, and Vrecl M (2007) Evidence for a role of caveolin-1 in neurokinin-1 receptor plasma-membrane localization, efficient signaling, and interaction with beta-arrestin 2. *Cell Tissue Res* **330:**231–245.
Kunapuli P and Benovic JL (1993) Cloning and expression of GRK5: a member of the G protein-coupled receptor kinase family. *Proc Natl Acad Sci U S A* **90:**5588–5592.
Li J, Xiang B, Su W, Zhang X, Huang Y, and Ma L (2003) Agonist-induced formation of opioid receptor-G protein-coupled receptor kinase (GRK)-G$\beta\gamma$ complex on membrane is required for GRK2 function in vivo. *J Biol Chem* **278:**30219–30226.
Liu JJ, Hartman DS, and Bostwick JR (2003) An immobilized metal ion affinity adsorption and scintillation proximity assay for receptor-stimulated phosphoinositide hydrolysis. *Anal Biochem* **318:**91–99.
Luttrell LM and Lefkowitz RJ (2002) The role of beta-arrestins in the termination and transduction of G-protein-coupled receptor signals. *J Cell Sci* **115:**455–465.
Marullo S and Bouvier M (2007) Resonance energy transfer approaches in molecular pharmacology and beyond. *Trends Pharmacol Sci* **28:**362–365.
Mercier JF, Salahpour A, Angers S, Breit A, and Bouvier M (2002) Quantitative assessment of β_1- and β_2-adrenergic receptor homo- and heterodimerization by bioluminescence resonance energy transfer. *J Biol Chem* **277:**44925–44931.
Milligan G (2004) Applications of bioluminescence- and fluorescence resonance energy transfer to drug discovery at G protein-coupled receptors. *Eur J Pharm Sci* **21:**397–405.
Nishimura K, Warabi K, Roush ED, Frederick J, Schwinn DA, and Kwatra MM (1998) Characterization of GRK2-catalyzed phosphorylation of the human substance P receptor in Sf9 membranes. *Biochemistry* **37:**1192–1198.
Oakley RH, Laporte SA, Holt JA, Barak LS, and Caron MG (2001) Molecular determinants underlying the formation of stable intracellular G protein-coupled receptor-β-arrestin complexes after receptor endocytosis. *J Biol Chem* **276:**19452–19460.
Palczewski K, Kumasaka T, Hori T, Behnke CA, Motoshima H, Fox BA, Le T, I, Teller DC, Okada T, et al. (2000) Crystal structure of rhodopsin: a G protein-coupled receptor. *Science* **289:**739–745.
Pao CS and Benovic JL (2002) Phosphorylation-independent desensitization of G protein-coupled receptors? *Sci STKE* **2002:**E42.
Perroy J, Pontier S, Charest PG, Aubry M, and Bouvier M (2004) Real-time monitoring of ubiquitination in living cells by BRET. *Nat Methods* **1:**203–208.
Pitcher JA, Inglese J, Higgins JB, Arriza JL, Casey PJ, Kim C, Benovic JL, Kwatra MM, Caron MG, and Lefkowitz RJ (1992) Role of beta gamma subunits of G proteins in targeting the beta-adrenergic receptor kinase to membrane-bound receptors. *Science* **257:**1264–1267.
Premont RT, Koch WJ, Inglese J, and Lefkowitz RJ (1994) Identification, purification, and characterization of GRK5, a member of the family of G protein-coupled receptor kinases. *J Biol Chem* **269:**6832–6841.
Pronin AN and Benovic JL (1997) Regulation of the G protein-coupled receptor kinase GRK5 by protein kinase C. *J Biol Chem* **272:**3806–3812.
Pronin AN, Satpaev DK, Slepak VZ, and Benovic JL (1997) Regulation of G protein-coupled receptor kinases by calmodulin and localization of the calmodulin binding domain. *J Biol Chem* **272:**18273–18280.
Ren XR, Reiter E, Ahn S, Kim J, Chen W, and Lefkowitz RJ (2005) Different G protein-coupled receptor kinases govern G protein and beta-arrestin-mediated signaling of V2 Vasopressin Receptor. *Proc Natl Acad Sci U S A* **102:**1448–1453.
Richardson MD, Balius AM, Yamaguchi K, Freilich ER, Barak LS, and Kwatra MM (2003) Human substance P receptor lacking the C-terminal domain remains competent to desensitize and internalize. *J Neurochem* **84:**854–863.
Schulz R, Wehmeyer A, and Schulz K (2002) Opioid receptor types selectively cointernalize with G protein-coupled receptor kinases 2 and 3. *J Pharmacol Exp Ther* **300:**376–384.
Shetzline MA, Premont RT, Walker JK, Vigna SR, and Caron MG (1998) A role for receptor kinases in the regulation of class II G protein-coupled receptors. Phosphorylation and desensitization of the secretin receptor. *J Biol Chem* **273:**6756–6762.
Shetzline MA, Walker JK, Valenzano KJ, and Premont RT (2002) Vasoactive intestinal polypeptide type-1 receptor regulation. Desensitization, phosphorylation, and sequestration. *J Biol Chem* **277:**25519–25526.
Thiyagarajan MM, Stracquatanio RP, Pronin AN, Evanko DS, Benovic JL, and Wedegaertner PB (2004) A predicted amphipathic helix mediates plasma membrane localization of GRK5. *J Biol Chem* **279:**17989–17995.
Tiruppathi C, Yan W, Sandoval R, Naqvi T, Pronin AN, Benovic JL, and Malik AB (2000) G protein-coupled receptor kinase-5 regulates thrombin-activated signaling in endothelial cells. *Proc Natl Acad Sci U S A* **97:**7440–7445.
Vrecl M, Jorgensen R, Pogacnik A, and Heding A (2004) Development of a BRET2 screening assay using beta-arrestin 2 mutants. *J Biomol Screen* **9:**322–333.
Walker JK, Premont RT, Barak LS, Caron MG, and Shetzline MA (1999) Properties of secretin receptor internalization differ from those of the β_2-adrenergic receptor. *J Biol Chem* **274:**31515–31523.

Address correspondence to: Christian E. Elling, 7TM Pharma A/S, 2970 Horsholm, Denmark. E-mail: cee@7tm.com